Optimizing Methanol Flow Rate for Enhanced Semi-Passive Mini-Direct Methanol Fuel Cell Performance

Laura Faria and V.María Barragán *

Posted Date: 11 January 2025

doi: 10.20944/preprints202501.0827.v1

Keywords: semi passive mode; DMFC; cell performance; methanol crossover; methanol flow; experimental study

Article

Optimizing Methanol Flow Rate for Enhanced Semi-Passive Mini-Direct Methanol Fuel Cell Performance

Laura Faria and V.María Barragán *

Department of Structure Matter, Thermal Physics and Electronics, Faculty of Physics, Complutense University of Madrid, Spain

* Correspondence: vmabarra@ucm.es

Abstract: A parametric experimental study was carried out to study the influence of temperature (25-40°C), concentration (0.15-6 wt. % methanol in water) and rate of the methanol flow (1.12-8.65 g/s) on the performance of a single mini-direct methanol fuel cell (DMFC) operating in semi passive mode with passive cathode and active anode. Open circuit voltage, maximum power density and cell efficiency were analyzed. To this purpose, open circuit voltage and current-voltage curves were measured in different experimental conditions. Results indicate that temperature is the most decisive parameter to increase DMFC performance. The performance increases with operation temperature, independently of the concentration and rate of the methanol flow. However, the impact of the concentration and flow rate depends on the value of the other parameters. The operating optimal concentration was 1 %wt. The results show that switching from passive to semi-passive mode improves fuel cell performance, but a subsequent increase in flow rate leads to a decrease in performance. An optimum value of the flow rate is observed dependent on methanol flow temperature and concentration.

Keywords: semi passive mode; DMFC; cell performance; methanol crossover; methanol flow; experimental study

1. Introduction

A direct methanol fuel cell (DMFC) is a type of fuel cell that directly converts the chemical energy found in methanol into electricity through an electrochemical reaction. Due to its high energy density, low emissions, and the ability to use a liquid fuel, this type of fuel cell has gained significant attention as a promising alternative energy source for portable and small-scale applications [1]. So, micro- and mini-DMFCs are promising technology [2–5]. In recent years, significant progress has been made in improving efficiency and performance of DMFCs, particularly through the development of new catalysts [6–8] and better electrolyte membranes with improved ionic conductivity [9–11]. Additionally, there have been advances in cost reduction and scalability by using cheaper materials and more efficient manufacturing methods [12]. The influence of operative parameters in the output performance has been also analysed [13–15] Despite the progress made, several challenges remain for DMFC technology [2]. Methanol transport passing through the membrane from the anode to the cathode, known as methanol crossover, is one of the major issues concerning DMFC technology. This results in high fuel loss and leakage current due to the oxidation of methanol produced at the cathode, and several studies have been dedicated to analysing this problem [11,16–19]. Another significant issue occurring at the anode is the formation of CO_2 bubbles, which can eventually block the flow. Work has been devoted to understanding the flow dynamics [20–22].

Depending on the supply mode of the fuel and the oxidant to the fuel cell, DMFC systems can be categorized into active, semi-passive, or passive modes [2,23]. Passive mode is ideal for portable devices, as it does not require a fuel pump or active airflow, thus reducing system complexity and operational costs. However, this mode also presents some challenges, such as lower efficiency

 doi:10.20944/preprints202501.0827.v1

compared to active systems and a higher risk of unreacted methanol accumulation. This can lead to energy losses and lower efficiency if the operating conditions are not properly managed. In active mode, circulating systems are used to supply methanol and oxygen to the anode and cathode, respectively [23,24]. In semi-passive mode with an active anode, auxiliary components are necessary to supply fuel to the anode, while oxygen is directly taken from the ambient air surrounding the system.

Incorporating a circulation system for methanol in the anode of DMFCs offers several key advantages, such as a more uniform reactant distribution, better control of methanol concentration, minimized methanol loss and catalyst poisoning, and improve temperature control of the fuel cell. Moreover, it helps to remove CO_2 accumulation by extracting it from the reaction zone. A well-designed circulation system can enhance the performance and longevity of the DMFC. However, the use of a circulating system increases its complexity, and if the flow rate is not optimized, it may negatively impact DMFC performance. There has been a growing interest in active and semi-passive DMFCs [2,24–29]. Therefore, more research into these modes is required.

The purpose of this work is to study the effect of the methanol flow rate on the behaviour of a mini-direct methanol fuel cell in semi-passive mode, analysing the influence of temperature and methanol concentration in the search for operational conditions that optimize the cell performance.

2. Fundamentals of the DMFC

A direct methanol fuel cell (DMFC) is a type of fuel cell that uses a methanol water solution as fuel and a proton exchange membrane as electrolyte. The chemical reactions occurring within a DMFC are:

Anode	$CH_3OH + H_2O \rightarrow CO_2 + 6H^+ + 6e^-$	(a)
Cathode	$\frac{3}{2}O_2 + 6H^+ + 6e^- \rightarrow 3H_2O$	(b)
Overal reaction	$CH_3OH + \frac{3}{2}O_2 \rightarrow CO_2 + 2H_2O$	(c)

(1)

Polarization curves are an effective way of characterizing the performance of a fuel cell. The form of this curve shows the different voltage losses: activation, crossover, ohmic and concentration losses [30,31]. The equation for the actual cell voltage, considering the different losses, can be expressed as:

$$E_{cell} = E_r - E_{act} - E_{ohm} - E_{con} \quad (2)$$

where E_{act} takes into account both activation and crossover losses, E_{ohm} and E_{con} indicate, respectively, ohmic and concentration losses, and E_r indicates the fuel cell reversible voltage, which depends on the temperature and pressure.

Under various simplifications [31], Eq. (2) can be written as:

$$E_{cell} = E_r - \frac{RT}{\alpha F}\ln\left(\frac{i+i_{loss}}{i_0}\right) - iR_{fc} - \frac{RT}{nF}\ln\left(\frac{i_L}{i_L - i}\right) \quad (3)$$

where α and i_0, transfer coefficient and exchange current density, respectively, are parameters involved in activation losses, i_{loss} is the loss current due to crossover fuel and internal current, R_{fc} is the ohmic fuel cell resistance, involved in ohmic losses, and i_L is the limiting current density related to concentration polarization losses.

Operating conditions affect all the terms in Eq. (3). in a different way. E_r can be expressed as a function of temperature and partial pressure of the reactant, using the Nernst equation [32].

If all methanol is not completely oxidized in the anodic catalytic layer (Eq. 1a) before it can reach the membrane surface, it can pass through the membrane to the cathode side leading to fuel cell performance losses, an effect known as methanol crossover. In a direct methanol fuel cell, the main contribution to i_{loss} is generally due to the crossover methanol through the membrane.

 doi:10.20944/preprints202501.0827.v1

Figure 1 shows the different transport mechanisms in a direct methanol fuel cell operating in semi passive mode with liquid-feed. In this operating mode, the methanol-water solution is circulating in the anode compartment, and air is supplied to the cathode by natural convection. In the figure, the typical methanol concentration profile is also shown. Methanol and water transport through the anode diffusion layer by diffusion and convection to the catalytic layer, where the oxidation reaction takes place. If the proton exchange membrane (PEM) is not an ideal barrier to methanol, there will be a portion of unoxidized methanol which, together with water, which crosses the membrane towards the cathode catalytic layer. This transport, named crossover, can occur by means three mechanisms: electroosmotic drag by protons and diffusion and permeation due to, concentration and pressure gradients, respectively, established between both electrodes. A return flow to the anode, named back convection, may also occur. if the cathode pressure was larger than the anode pressure. However, in the semi passive mode with an active anode, the anode pressure will be larger than that in the cathode, so, the back convection mechanism is not expected to occur.

Thus, methanol permeates from the anode to the cathode through the membrane via diffusion, convection and electroosmosis, and methanol crossover flux can be expressed as:

$$J_{MeOH}^{crossover} = D\Delta c + K\Delta p + Wi \quad (4)$$

where D is related to the effective diffusivity of methanol in the membrane and its thickness, K with the effective hydraulic permeability and thickness of the membrane and viscosity of the solution, and W with the electroosmotic drag coefficient of water in the membrane. Δc and Δp are, respectively, the difference of concentration and pressure across the membrane, and i is the current density. This flux affects the actual cell voltage.

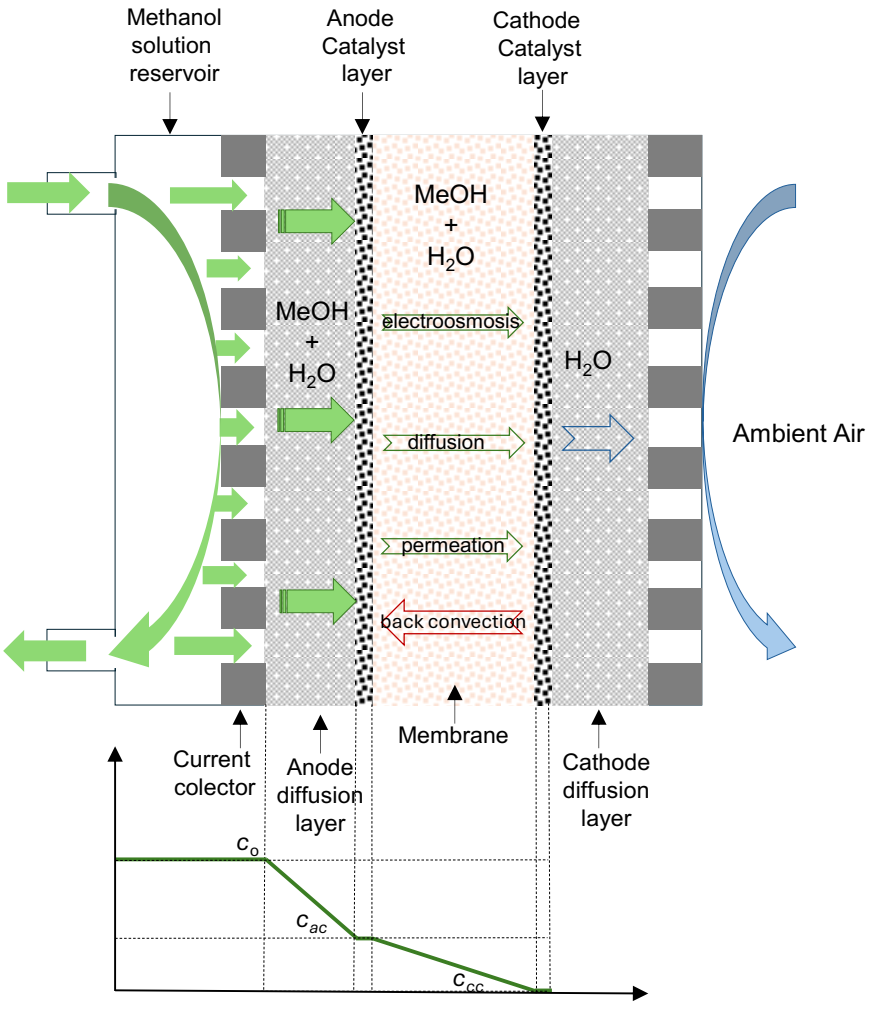

 doi:10.20944/preprints202501.0827.v1

Figure 1. Schematic diagram of the mass transport mechanism in a semi passive liquid-feed DMFC with active anode. (top of the figure) and typical methanol concentration profile in a DMFC (bottom of the figure). C_0 is the methanol solution concentration in the reservoir and c_{ac} and c_{cc} are, respectively, the concentrations in the anode and cathode catalyst layers.

Crossover also affects to the cell voltage at zero current, termed open circuit voltage (*OCV*), that, according to Eq. (3), can be expressed as:

$$OCV = E_r - \frac{RT}{\alpha F}\ln\left(\frac{i_{loss}}{i_0}\right) \quad (5)$$

Methanol crossover can be expressed as an equivalent crossover current density [17]. By supposing that the contribution of methanol crossover is the main contribution to the current loss, it can be expressed as:

$$i_{loss} = 6FJ_{MeOH}^{crossover} \quad (6)$$

According to Eqs. (4-6), at zero current, methanol crossover will depend on the concentration and pressure differences existing between anode and cathode and, so, on the anode methanol concentration and flow rate, affecting *OCV*. E_r also depends on the pressure, and it will be different at different anode inlet pressures. With liquid water and methanol, according to Eq. (1a), flow rate will affect to the CO_2 partial pressure in the anode compartment.

Under not zero currents, the electroosmotic contribution to methanol crossover will also affect the actual cell voltage.

3. Materials and Methods

A commercial single methanol fuel cell was used in this work. The electrodes were E-TEK, ELAT/VHL/DS/VS Double sided Version 2-ELAT with Pt-Ru Ox Power (1:1 a/o) catalyst with a loading of 5.0 mg/cm^2 on the anode, and EFCG electrode with Toray Carbon paper TGP-H-12o with Pt Black catalyst with a loading of 2.0g/cm^2 on the cathode. It uses a Nafion 115 membrane as electrolyte membrane

For the semi active mode operation, methanol fuel with five different concentrations (0.15, 0.5, 1, 3 and 6 %wt. methanol in water) was supplied at the anode by using a peristaltic pump which permitted to vary the flow rate. The temperature of the methanol fuel was controlled by means of a thermostat bath. To this end, the methanol-water solution was content in a glass balloon immersed in the bath and made circulated through the anode by means of the peristaltic pump which permitted to vary the flow rate up to 8.9g/s). Ambient air was supplied to the cathode. A fan was placed near the cathode to facilitate air flow towards the cathode side of the cell. Room temperature, pressure and relativity humidity were, respectively in the range 22-25°C, 930-950 hPa, and 30-40 %. Temperatures of the methanol fuel in the glass ballon, and of the cathode surface were measured during the experiment. An imagen of the experimental device is shown in Figure 2.

 doi:10.20944/preprints202501.0827.v1

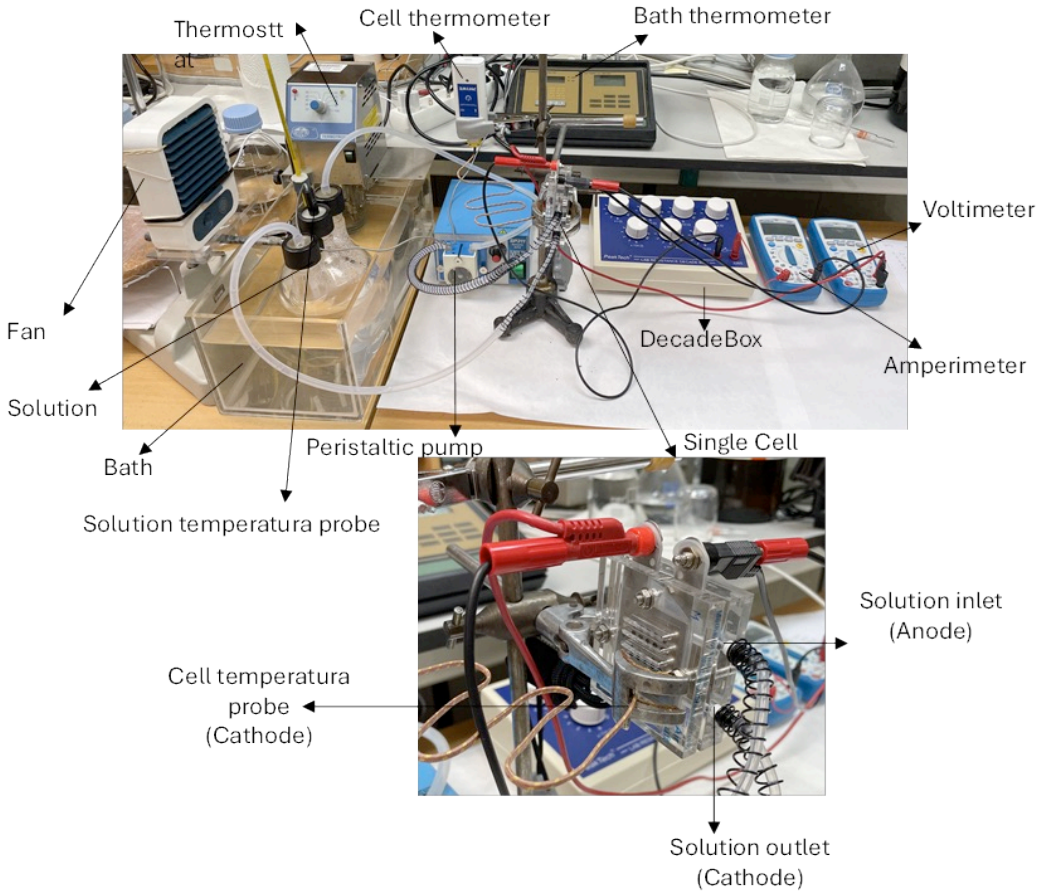

Figure 2. Experimental device used in this work. General view (top of the figure). Detail of the single cell (bottom of the figure).

Current (I) and voltage (E_{cell}) were measured under different loads to obtain the corresponding polarization curves. Open circuit voltage (OCV) was obtained as the voltage at zero current. The maximum power value was obtained from the corresponding power-current curve in each experimental situation.

The area of the membrane electrode assembly was 3x3 cm². However, due to the geometry of the channels of access to the diffusion layer, pin channel in our case (see Figure 3), the effective area was estimated at 1.56 cm².

Figure 3. Metal current collector of the fuel cell with a grid geometry.

4. Results and Discussion

 doi:10.20944/preprints202501.0827.v1

4.1. Peristaltic Pump Caracterization

To measure the inlet pressure in the anode due to the flow rate of the methanol feed, a pressure sensor was placed at the anode inlet. Figure 4 shows the measured values of the rate and pressure for each flow level of the pump. As can be observed, from level five, the flow rate was no longer significantly different, so measurements were made for five different flows up to this value (namely F1, F2, F3, F4 and F5). F0 corresponds to zero flow in passive mode. The inlet pressure increases with the flow rate. The small figure inside of Figure 4 shows pressure versus flow rate for the different flow levels.

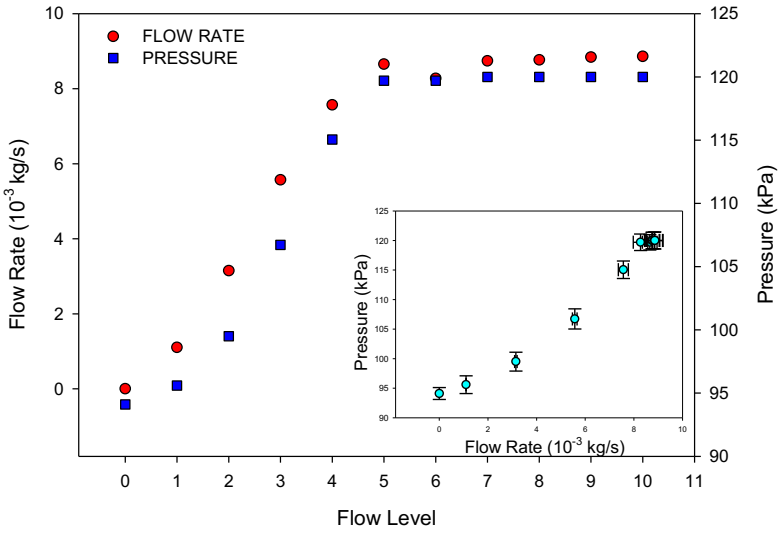

Figure 4. Flow rate and inlet pressure for the different flow levels of the peristaltic pump. The small figure inside shows the inlet pressure as a function of the flow rate.

As the pressure of the cathode was always the atmospheric pressure, it was always smaller than the anode pressure. Thus, semi passive mode would involve the existencce of a pressure difference between anode and cathode. This is a important key in relation to the methanol crossover effect.

4.2. Open Circuit Voltage

Open circuit voltage has been measured in different experimental conditions. Figure 5 shows the influence of the methanol flow rate at different concentrations for each temperature. The same scale has been used for all temperatures for a better comparison of the results.

 doi:10.20944/preprints202501.0827.v1

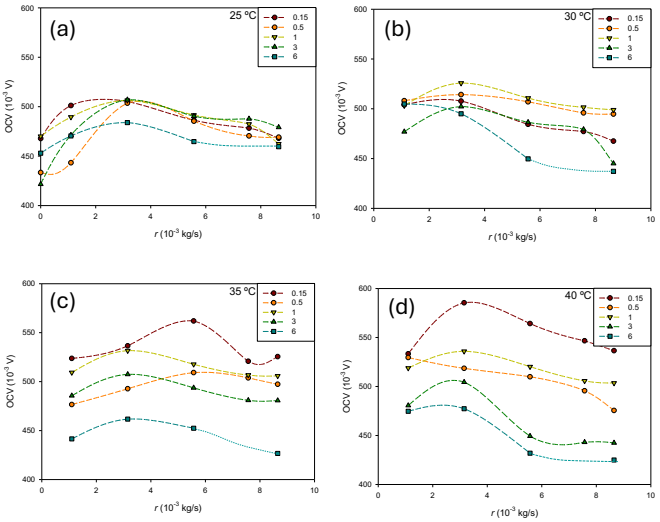

Figure 5. Open circuit voltage (*OCV*) as a function of the methanol flow rate (*r*) at different methanol concentrations (in wt. %) for each temperature. Discontinuous lines are only visual guides.

In general, the transition from passive to semi-passive mode increases the *OCV* at low methanol flow rates. As can be observed, the *OCV* is influenced by the methanol flow rate, but the relationship is not straightforward. It depends on both temperature and methanol concentration. The effect of concentration becomes more pronounced as the temperature increases. At 25°C (Figure 4a), the influence of the methanol concentration is lower at higher flows, while the opposite trend is observed at 40°C (Figure 4d). The accumulation of byproducts like CO_2 is expected to be greater in passive mode. The methanol flow facilitates efficient bubble detachment. However, the increase the methanol inlet velocity also may enlarge bubble detachment diameters, potentially causing segmental plugging Tong et al. [22] showed that optimal selection of the CO_2 inlet velocity facilitates effective bubble detachment. Moreover, as the flow rate increases, the pressure difference between the anode and cathode also increases, leading to a rise in transmembrane pressure difference. This, according to Eq. 4, results in greater methanol permeation through the membrane and increased mass transport losses. Consequently, an optimal flow rate is expected to exist. Overall, the effect of the flow rate on *OCV* can vary depending on specific operating conditions and cell design. Striking a balance is essential to maximize performance.

From Eq. (4), a β parameter can be defined as:

$$\beta = \frac{(E_r - OCV)F}{RT} = \frac{1}{\alpha}\ln\left(\frac{i_{loss}}{i_0}\right) \quad (6)$$

At a given concentration and temperature, β serves as an indicator of the change in *OCV* due to the influence of the anode inlet pressure in the activation and crossover losses. To estimate β values for each temperature and pressure, reversible voltages E_r were previously calculated using data from literature. These calculations consider the reaction enthalpy and entropy at 25°C and atmospheric pressure, the temperature dependence of the specific heat of the reaction components, and the pressure effect as described by the Nernst equation [31]. The results are presented in Table 1.

Table 1. Reversible voltage E_r at different pressures and temperatures[1].

Flow level	Inlet Pressure (kPa)	25°C	30°C	35°C	40°C
F1	95.6	1.2027	1.1340	1.0604	0.9817
F2	99.5	1.2025	1.1338	1.0603	0.9815
F3	106.7	1.2022	1.1335	1.0599	0.9812
F4	115.0	1.2019	1.1332	1.0596	0.9808

 doi:10.20944/preprints202501.0827.v1

F5	119.7	1.2017	1.1330	1.0594	0.9807

[1]Liquid water and methanol have been considered.

As can be observed, reversible voltage decreases with increasing temperature. At a given temperature, an increase in the anode pressure also reduces the reversible voltage. Using data in Table 1 and Eq. (6), values of β has been estimated under all conditions. The results are shown in Figure 6.

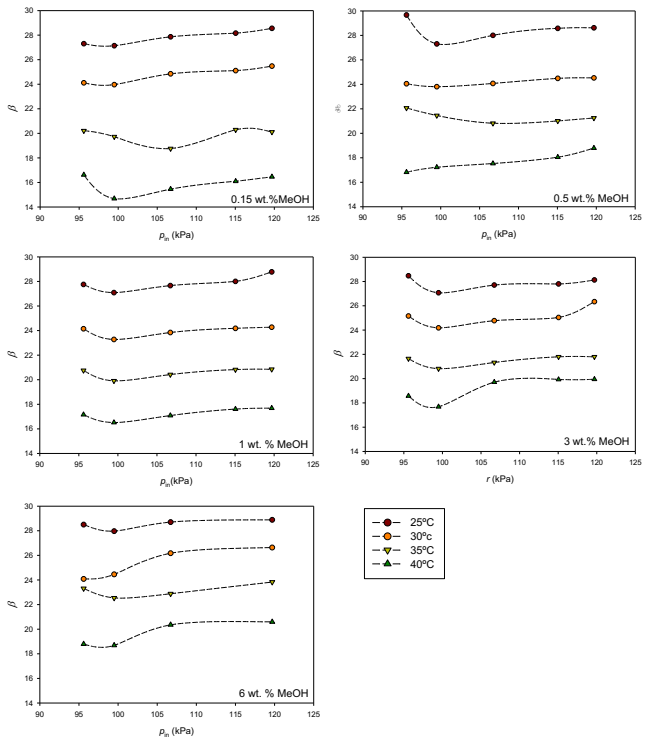

Figure 6. Parameter β as a function of anode inlet pressure at different methanol concentrations (in wt. %) for each temperature. Discontinuous lines are only visual guides.

Considering Eq. (6), the dependence of parameter β on the inlet pressure must arise from the dependence of α, i_{loss} and i_0 on the pressure. In general, the observed trend is similar across temperatures and concentrations. Beyond a certain flow level, parameter β increases with rising pressure. For the analyzed system, the effect of the inlet pressure becomes harmful, in general, when the anode pressure exceeds the cathode pressure by approximately 5-6 kPa.

4.3. Polarization Curves.

Current-voltage curves at different flow rates have been measured for each concentration and temperature. From them, the corresponding current-power curves were obtained. Figure 7 presents the results obtained for all the systems. The same axes scale has been used across all figures, where possible, to facilitate comparison of the results.

 doi:10.20944/preprints202501.0827.v1

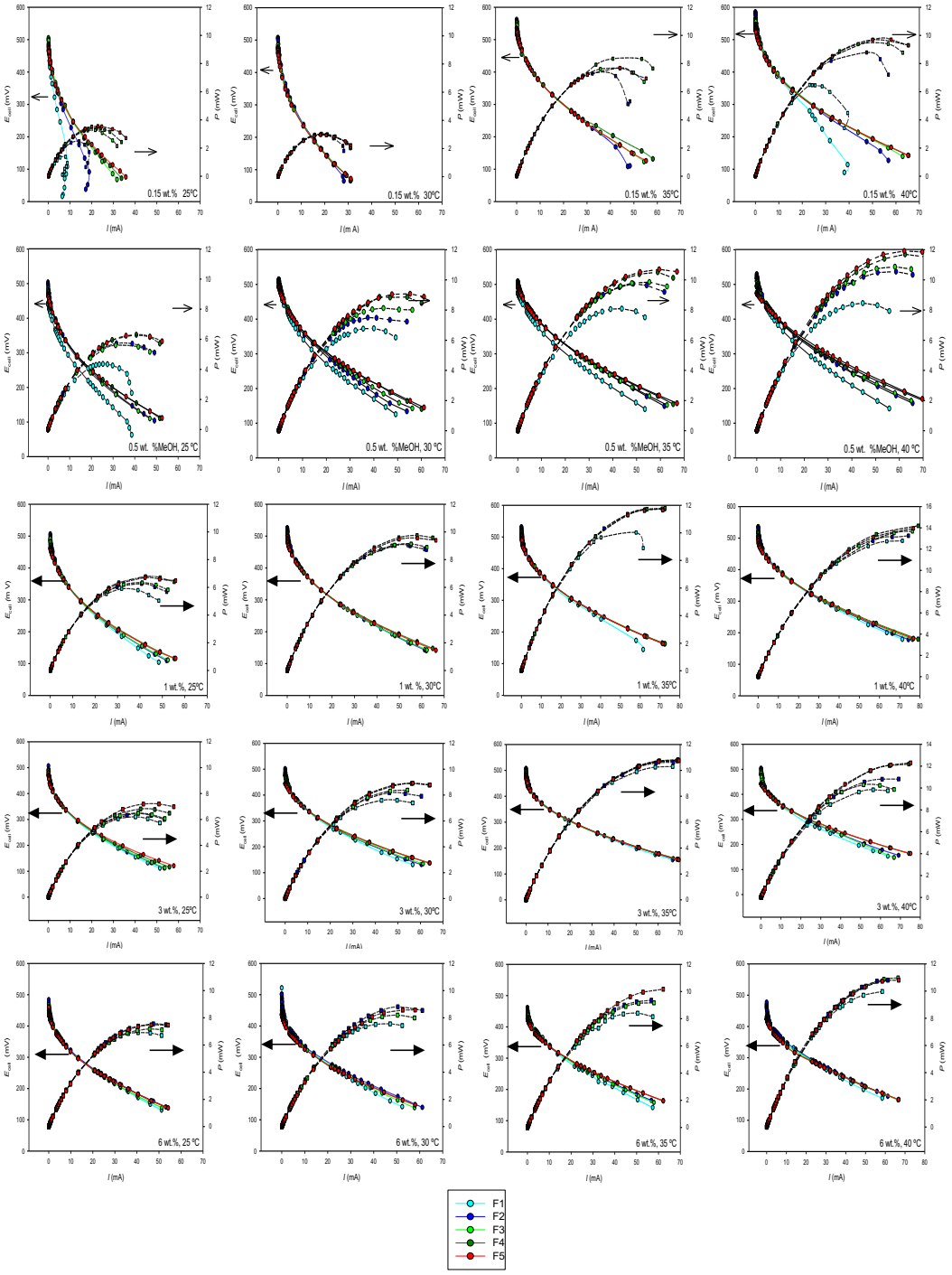

Figure 7. Current-voltage and current-power curves at different methanol flow rates for all the concentration and temperatures analysed in this work. Lines are only visual guides.

As observed, both temperature and methanol concentration influence the profiles of the current-voltage curves. Generally, higher currents are achieved at elevated temperatures, consistent with previous findings in the literature [14]. The effect of concentration depends on both temperature and flow rate. We observed that, at low concentrations, an increase in concentration results in higher currents, particularly at low flow rates. However, at the highest concentrations, the opposite effect is observed, depending on the flow rate. Using mini-direct methanol fuel cells in passive mode, Colmati et al. [5] found that methanol concentrations near 2 mol l^{-1} gave the highest current levels. They observed, however, that using methanol concentrations above 5 mol/l, the performance of the mini-cell dropped, probably because the crossover of methanol increased too much.

 doi:10.20944/preprints202501.0827.v1

The most significant effect of the flow rate occurs at higher currents. In this region, the flow rate has a greater influence, especially at lower concentrations, with higher currents observed at higher flow rates.

The effect of the operating parameters can also be examined by analyzing the corresponding current-power curves, also shown in Figure 7. Cell power increases with current until the maximum value is reached. At a given methanol concentration, cell power increases with temperature. It is also evident that the effect of temperature is more pronounced at lower methanol concentrations. At a specific temperature, the influence of methanol concentration varies depending on its value. This effect will be further discussed in relation to the maximum power output of the cell. Regarding the impact of methanol flow rate, it is observed that its influence is more significant at lower methanol concentrations. As concentration increases, the differences between the curves at varying flow rates become less pronounced.

4.4. Maximum Power Density.

From the current-power curves, the maximum power density supplied by the cell under different experimental conditions was determined. The results are shown in Figure 8, where the same axis scale has been used to facilitate comparison.

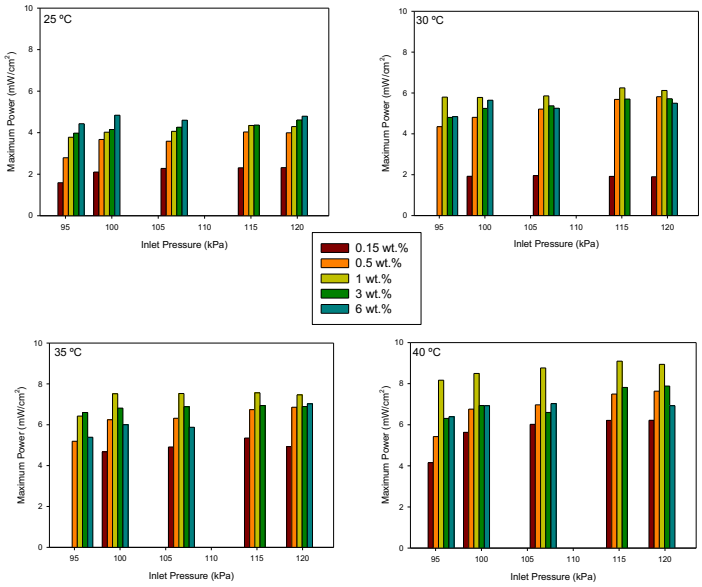

Figure 8. Maximum power density as a function of the inlet pressure at different methanol concentrations and temperatures.

It is observed that, for all methanol concentrations, the maximum power density increases with temperature. However, the effect of concentration varies depending on the temperature. A concentration increase reduces resistance loss and concentration polarization effects, but methanol crossover increases. Membrane methanol diffusion and hydraulic permeability increase with temperature [11]. Therefore, an optimal concentration value is expected.

Table 2 presents the maximum power density values at ambient temperature (25°C) for each concentration, along with the corresponding flow rates. At 25°C, an increase in concentration results in a higher maximum power density, but this maximum value is observed at lower flow rates as the concentration increases.

Table 2. Optimal level flow and maximum power values obtained for each methanol concentration at ambient temperature.

Methanol	Anode	Flow	Pressure	Maximum

 doi:10.20944/preprints202501.0827.v1

concentration (wt.%)	temperature (°C)	level	difference (kPa)[1]	power density (mW/cm²)
0.15	25	F5	26	2.3
0.5	25	F4	21	4.0
1	25	F4	21	4.3
3	25	F5	26	4.6
6	**25**	**F2**	**5**	**4.8**

At ambient temperature, the higher value for the maximum power density was observed at a methanol concentration of 6 wt.% and flow level F2.

Table 3 presents the maximum power densities and their corresponding operating parameters for each methanol concentration. As shown, the highest value was achieved at the highest temperature, but with 1 wt.% concentration

Table 3. Optimal operating parameters and maximum power densities obtained for each methanol concentration.

Methanol concentration (wt.%)	Anode temperature (°C)	Flow level	Pressure difference (kPa)[1]	Maximum power density (mW/cm²)
0.15	40	F5	26	6.2
0.5	40	F5	26	7.6
1	**40**	**F4**	**21**	**9.1**
3	40	F4	21	7.9
6	40	F3	13	7.0

These results suggest that the optimal flow level and, consequently, the optimal pressure difference between the anode and cathode, depends on the other operating parameters.

4.5. Maximum Efficiency

With the purpose of examining efficiency under the conditions of maximum power, the efficiency values were estimated for 1 and 6 wt. % methanol concentrations according to the following expression:

$$\eta = \left(\frac{E_{cell}}{E_{th}}\right)\left(\frac{i}{i + i_{loss}}\right) \quad (7)$$

where *Eth* indicates the thermoneutral potential, which can be calculated from the corresponding reaction enthalpy values. The values of i_{loss} were estimated from voltage-current curves at low currents by fitting experimental values to Eq. (3). We assumed that, at very low currents, ohmic and polarization losses could be neglected. Transfer coefficients close to unity were obtained in all cases. The values of the loss current were of the order of 10^{-3} A, and for the exchange current, values of the order of 10^{-5} A were obtained. The results are shown in Figure 9.

 doi:10.20944/preprints202501.0827.v1

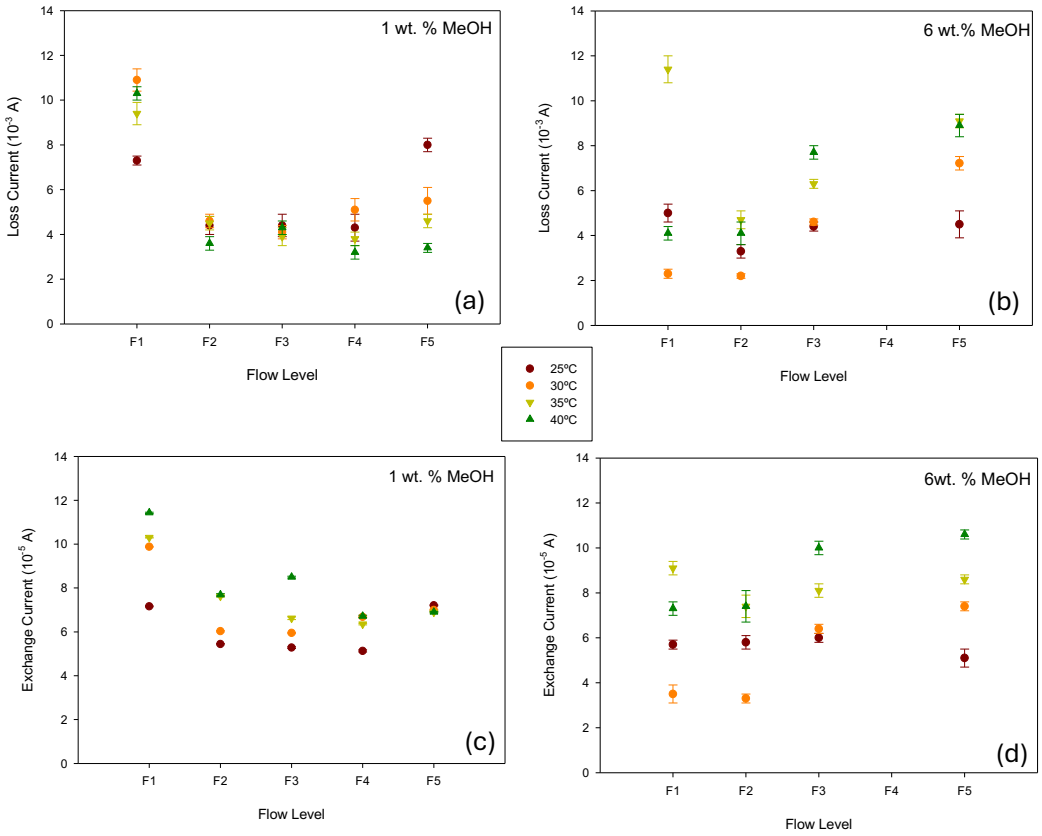

Figure 9. Values for the loss and exchange currents estimated from fitting experimental values to Equation (3).

Although the effect of the methanol flow rate on the loss current depends on the anode methanol concentration, it is observed that increasing the flow reduces the loss current, likely due to the more uniform distribution of methanol. However, as the flow rate increases, the anode pressure also rises, which in turn favours methanol crossover. A minimum value for the loss current is observed at intermediate flow rates, which is more noticeable at a 6 wt. % concentration, where the crossover effect is greater.

Figure 10 shows the efficiency-current curves obtained for 1 and 6 wt. % at the different temperatures and flow rates. The maximum efficiency value for each flow rate and temperature is also shown. As can be seen, both methanol concentration and temperature influence the effect of the flow rate on cell efficiency.

 doi:10.20944/preprints202501.0827.v1

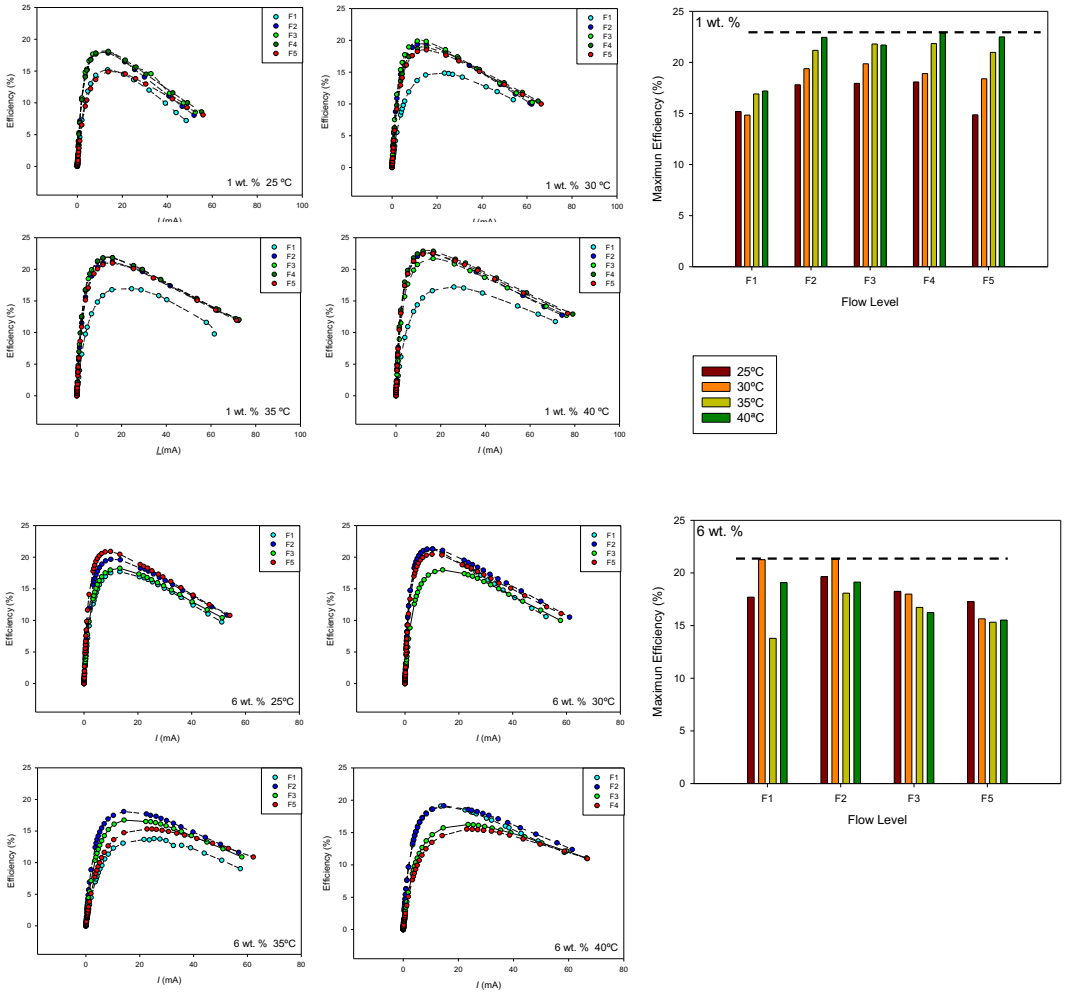

Figure 10. Efficiency-current curves (left) and maximum efficiency values (right) as a function of the flow level at different temperatures for 1 and 6 wt. % methanol concentrations.

At 1 wt. % methanol concentration, higher efficiencies were obtained at higher temperatures. The maximum cell efficiency was also observed at flow level F4. At 6 wt. % methanol concentration, the maximum efficiency was observed at 30°C and flow level F2. In this case, an increase in flow rate and temperature leads to lower efficiency values, probably due to an increase in the methanol crossover effect.

5. Conclusions

A mini-direct methanol fuel cell operating in semi-passive mode with an open cathode were evaluated. The influence of the anode methanol flow rate on open-circuit voltage, maximum power, and fuel efficiency of the cell was analysed for different methanol concentrations and temperatures.

The results show that, in general, switching from passive to semi-passive mode increases the open-circuit voltage and cell power, improving fuel cell performance. However, a subsequent increase in the flow rate leads to a decrease in performance. An optimal flow rate value was observed, depending on methanol flow temperature and concentration.

At ambient temperature, maximum power was observed with the higher methanol concentration and low flow rate. However, at higher temperatures, under the operating conditions analysed (25-40°C and 0.15-6 wt. %), the maximum power was observed for a methanol concentration of 1 wt. % and 40°C. Under these operating conditions, the fuel cell also showed maximum efficiency.

 doi:10.20944/preprints202501.0827.v1

The results seem to indicate that methanol circulation at low flow rates has a positive effect on fuel cell performance, probably because it enhances the uniform distribution of the reactant, reducing localized accumulation and improving the electrochemical reaction. Additionally, circulation can help remove CO_2 produced during methanol oxidation, avoiding the formation of concentration gradients.

However, a subsequent increase in flow rate leads to a decrease in fuel cell performance, depending on concentration and temperature. This may be due to the methanol circulation causing a pressure difference between the anode and cathode, which favours the methanol crossover effect. This effect is more pronounced at higher temperatures and concentrations, probably due to higher temperature and concentration favour methanol crossover.

Proper management of the anode flow is necessary, depending on temperature and methanol concentration.

Author Contributions: "Conceptualization, V.M.B.; methodology, L.F. and V.M.B.; software, L.F. and V.M.B.; validation, V.M.B. and L.F.; formal analysis, L.F. and V.M.B.; investigation, V.M.B.; resources, V.M.B.; data curation, L.F. and V.M.B.; writing—original draft preparation, V.M.B.; writing—review and editing, L.F. and V.M.B.; visualization, L.F.; supervision, V.M.B.; All authors have read and agreed to the published version of the manuscript.

Funding: This research received no external funding.

Data Availability Statement: All the data included in this study is presented in the manuscript.

Conflicts of Interest: The authors declare no conflicts of interest.

Abbreviations

The following abbreviations are used in this manuscript:

DMFC	Direct methanol fuel cell
MeOH	Methanol
OCV	Open Circuit Voltage
PEM	Proton exchange membrane

References

1. Ahmed, A.A.; Labadidi, M.A.; -Hamadg, A.T.; Orhan, M.F. Design and Utilization of a Direct Methanol Fuel Cell, *Membranes,* **2022**, *12*, 1266.
2. Falcão, D.S.; Olivera, V.B.; Rangel, C.M.; Pinto, A.M.F.R. Review on micro-direct methanol fuel cells, *Renewable and Sustainable Energy Rev.* **2014**, *34*, 58-70.
3. Moreira, C.S.; Pinto, A.M.F.R.; Oliveira, V.B. The effect of a reduction in the catalyst loading o mini passive direct methanol fuel cell. *Energies*, **2024**, *17*,5174.
4. Chen, X.; Zhang, Z.; Shen, J.; Hu, Z. Micro direct methanol fuel cell: functional components, supplies management, packaging technology and application, *Int. J. Energy Res*. **2017**, *41*, 613-627.
5. Colmati, F.; Paganin, V.A.; González, E.R. Effect of operational parameters of mini-direct methanol fuel cells operating at ambient temperature, *J. Appl. Electrochem*. **2006**, *36*, 17-23.
6. Mansor, M.; Timmiati, S.N.; Lim, K.L.; Wong, W.Y.; Kamarudin, S.K.; Kamarudin, N.H.N. Recent progress of anode catalysts and their support materials for methanol electrooxidation reaction, *Int. J. Hydrogen Energy*, **2019**, *44*, 14744-14769.
7. Chen, F.; Sun, Y.; Li, H.; Li, C, Review and Development of Anode Electrocatalyst Carrier for Direct Methanol Fuel Cells. *Energy Technol.*, **2022**, *10*, 2101086.
8. Tian, X.L.; Wang, L.; Deng, P.; Chen, Y.; Xia, B.Y. Research advances in unsupported Pt-based catalyst for electrochemical methanol oxidation, *J. Energy Chem*. **2017**, *26*, 1067-1078.
9. Junoh, H.; Jaafar, J.; Nordin, N.A.; Ismail, A.F.; Othman, M.H.D.; Rahman, M.A.; Aziz, F.; Yusof, N. Methanol fuel cell applications: Perspective on morphological structure, *Membranes*. **2020**, *10*, 34.

10. Kristskaya, D.A.; Novikova, K.S.; Sanginov, E.A.; Ponomarev, A.N. Testing of Polymer film-sulfonated polystyrene proton-exchange composite membranes in a direct methanol fuel cell at 60°C, *Membr. Membr. Technol.* **2024**, *6*,112-119.
11. Sun, X.; Yang, C.; Xia, Z.; Qi, F.; Syn, H., Sun, G. Molecular sieve as an effective barrier for methanol crossover in direct methanol fuel cells, *Int. J. Hydrogen Energy*. **2020**,*45*, 8994-9003.
12. Falcão, D.S.; Silva, R.A.; Rangel, C.M.; Pinto, A.M.F.R. Performance of an Active Micro direct Methanol Fuel Cell Using Reduced Catalyst Loading MEAs, *Energies*. **2017**, *10*, 1683.
13. Wang, Y.; Lu, Z.; Li, Y.; Ma, Z.; Gu, Y.; Guo, Q. Performance analysis and multi-optimization of direct methanol fuel cell based on a novel numerical model considering mass transfer, *Int. J. Hydrogen Energy*. **2024,** *62*, 362-374.
14. Govindarasu, R.; Somasundaram, S. Studies on Influence of Cell Temperature in Direct Methanol Fuel Cell Operation, Processes.**2020**, *8*, 353.
15. Yan, X.H.; Gao, P.; Zhao, G.; Shi, L.; Xu, J.B.; Zhao, T.S. Transport of highly concentrated fuel in direct methanol fuel cells, *Appl. Therm. Eng.* **2017**, *126*, 290-295.
16. Heinze, A.; Barragán, V.M. A review of the state-of-the-art of the methanol crossover in direct methanol fuel cells, *J. Power Sources*. **1999**, *84*, 70-74.
17. Barragán, V.M.; Heinzel, A. Estimation of the membrane methanol diffusion coefficient from open circuit voltage measurements in a direct methanol fuel cell, *J. Power Sources*. **2002**, *104*, 66-72.
18. Ji, F.; Yang, L.; Sun, H.; Wang, S.; Li, H.; Jiang, L.; Sun, G. A novel method for analysis and prediction of methanol mass transfer in direct methanol fuel cell, *Energy Conver. Manage.* **2017**, *154*, 482-490.
19. Xu, C.; Faghri, A.; Li, X.; Ward, T. Methanol and water crossover in a passive liquid-feed direct methanol fuel cell, *Int. J. Hydrogen Energy*. **2010**, *35*,1769-1777.
20. Weibin, Y.; Xiao, Z.; Zhang, W.; Ma, Q.; Li, Z.; Yan, X.; Su, H.; Xing, L.; Xu, Q. Influence of Current Collector Desing and Combination on the Performance of Passive Direct Methanol Fuel Cells, *Catalysts*. **2024**, *14*, 632.
21. Wang, S.; Zhang, X.; Xhang, N.L.; Liu, X. Elimination of water flooding of cathode current collector of micro passive direct methanol fuel cell by superhydrophilic surface treatment, *Appl. Energy*, **2014**,*126*, 107-112.
22. Tong, Y.; Thou, H.; Tian, Z.; Zhu, J.; Zhu, J. Analysis of CO2 bubble growth detachment kinetics in direct methanol fuel cell flow channels, *J. Power Sources*. **2025**, *628*, 235880.
23. Alias, M.S.; Kamarudin, S.K.; Zainoodin, A.M.; Masdar, M.S. Active direct methanol fuel cell: An overview, *Int. J. Hydrogen Energy*. **2020**,*45*, 19620-19641.
24. Li, X.; Miao, Z.; Marten, L. Blankenau, I. Experimental measurements of fuel and water crossover in an active DMFC, *Int. J. Hydrogen Energy*. **2021**,*46*, 4437-4446.
25. Ramasamy, J.; Palaniswamy, K.; Kumaresan, T.; Chandran, M.; Chen, R. Study of novel flow channels influence on the performance of direct methanol fuel cell, *Int. J. Hydrogen Energy*. **2022**,*47*, 595-609.
26. Calabriso, A.; Borello, D.; Romano, G. P.; Cedola, L.; Del Zotto, L. Bubbly flow mapping in the anode channel of a direct methanol fuel cell via PIV investigation, *Appl. Energy*, **2017**, *185*, 1245-1255.
27. Murmu, R.; Roy, D.; Sutar, H. Mathematical Modelling and Simulations of Active Direct Methanol Fuel Cell, *J. Polym. Mater*. **2023**, *40*, 125-139.
28. Lee, J.; Lee, S.; Han, D., Gwak, G.; Ju, H. Numerical modelling and simulations of active direct methanol fuel cell (DMFC) system under various ambient temperatures and operating conditions, *Int. J. Hydrogen Energy*. **2017**,*42*, 1736-1750.
29. Zhang, D.; Liu, Y.; Zhao, Z. Adaptive Joint Multiobjective Operating Parameters' Optimization for Active Direct Methanol Fuel Cells, *Energy Technol.* **2024**, *12*, 2300897.
30. O´Hayre, R.; Cha, S-W.; Colella, W.; Prinz, F.B. *Fuel Cell Fundamentals*, 2nd ed.; Wiley: New York, USA, 2009.
31. Barber, F. *PEM Fuel Cells: Theory and Practice*, Elsevier Academic Press: San Diego, USA, 2005.
32. Bockris, J. O´M.; Reddy, A.K.N.; Gamboa-Aldeco, M. *Modern Electrochemistry 2A,* 2nd ed.; Kluwer Academic: New York, USA, 2000,

 doi:10.20944/preprints202501.0827.v1

disclaim responsibility for any injury to people or property resulting from any ideas, methods, instructions or products referred to in the content.